

# Testing superscaling predictions in electroweak excitations of nuclei

M. Martini<sup>1</sup>, G. Co' <sup>1</sup>, M. Anguiano<sup>2</sup> and A. M. Lallena<sup>2</sup>

1) Dipartimento di Fisica, Università di Lecce and  
Istituto Nazionale di Fisica Nucleare sez. di Lecce,  
I-73100 Lecce, Italy

2) Departamento de Física Atómica, Molecular y Nuclear,  
Universidad de Granada, E-18071 Granada, Spain

December 18, 2006

## Abstract

Superscaling analysis of electroweak nuclear response functions is done for momentum transfer values from 300 to 700 MeV/c. Some effects, absent in the Relativistic Fermi Gas model, where the superscaling holds by construction, are considered. From the responses calculated for the  $^{12}\text{C}$ ,  $^{16}\text{O}$  and  $^{40}\text{Ca}$  nuclei, we have extracted a theoretical universal superscaling function similar to that obtained from the experimental responses. Theoretical and empirical universal scaling functions have been used to calculate electron and neutrino cross sections. These cross sections have been compared with those obtained with a complete calculation and, for the electron scattering case, with the experimental data.

## 1 Introduction

The properties of the Relativistic Fermi Gas (RFG) model of the nucleus [1] have inspired the idea of superscaling. In the RFG model, the responses of the system to an external perturbation are related to a universal function of a properly defined scaling variable which depends upon the energy and the momentum transferred to the system. The adjective universal means that the scaling function is independent on the momentum transfer, this is called scaling of first kind, and it is also independent on the number of nucleons, and this is indicated as scaling of second kind. The scaling function can be defined in such a way to result independent also on the specific type of external one-body operator. This feature is usually called scaling of zeroth-kind [2, 3, 4]. One has superscaling when the three kinds of scaling are verified. This happens in the RFG model.

The theoretical hypothesis of superscaling can be empirically tested by extracting response functions from the experimental cross sections and by studying their scaling behaviors. Inclusive electron scattering data in the quasi-elastic region have been analyzed in this way [2, 5]. The main result of these studies is that the longitudinal

responses show superscaling behavior. The situation for the transverse responses is much more complicated.

The presence of superscaling features in the data is relevant not only by itself, but also because this property can be used to make predictions. In effect, from a specific set of longitudinal response data [6], an empirical scaling function has been extracted [2], and has been used to obtain neutrino-nucleus cross sections in the quasi-elastic region [3].

We observe that the empirical scaling function is quite different from that predicted by the RFG model. This indicates the presence of physics effects not included in the RFG model, but still conserving the scaling properties. We have investigated the superscaling behavior of some of these effects. They are: the finite size of the system, its collective excitations, the Meson Exchange Currents (MEC) and the Final State Interactions (FSI). The inclusion of these effects produce scaling functions rather similar to the empirical one. Our theoretical universal scaling functions,  $f_U^{\text{th}}$ , and the empirical one  $f_U^{\text{ex}}$ , have been used to predict electron and neutrino cross sections.

## 2 Superscaling beyond RFG model

The definitions of the scaling variables and functions, have been presented in a number of papers [1, 2, 3, 4] therefore we do not repeat them here. The basic quantities calculated in our work are the electromagnetic, and the weak, nuclear response functions. We have studied their scaling properties by direct numerical comparison (for a detailed analysis see Ref. [7]).

We present in Fig. 1 the experimental longitudinal and transverse scaling function data for the  $^{12}\text{C}$ ,  $^{40}\text{Ca}$  and  $^{56}\text{Fe}$  nuclei given in Ref. [6] for three values of the momentum transfer. We observe that the  $f_L$  functions scale better than the  $f_T$  ones. The  $f_T$  scaling functions of  $^{12}\text{C}$ , especially for the lower  $q$  values, are remarkably different from those of  $^{40}\text{Ca}$  and  $^{56}\text{Fe}$ .

The observation of the figure, indicates that the scaling of first kind, independence on the momentum transfer, and of zeroth kind, independence on the external probe, are not so well fulfilled by the experimental functions. These observations are in agreement with those of Refs. [2, 5].

To quantify the quality of the scaling between a set of  $M$  scaling functions, each of them known on a grid of  $K$  values of the scaling variable  $\Psi$ , we define the two indexes:

$$\mathcal{D} = \max_{i=1,\dots,K} \left\{ \max_{\alpha=1,\dots,M} [f_{\alpha}(\Psi_i)] - \min_{\alpha=1,\dots,M} [f_{\alpha}(\Psi_i)] \right\}, \quad (1)$$

and

$$\mathcal{R} = \frac{1}{K f^{\text{max}}} \sum_{i=1,\dots,K} \left\{ \max_{\alpha=1,\dots,M} [f_{\alpha}(\Psi_i)] - \min_{\alpha=1,\dots,M} [f_{\alpha}(\Psi_i)] \right\} \quad (2)$$

where  $f^{\text{max}}$  is the largest value of the  $f_{\alpha}$ .

The two indexes give complementary information. The  $\mathcal{D}$  index is related to a local property of the functions: the maximum distance between the various curves. Since the

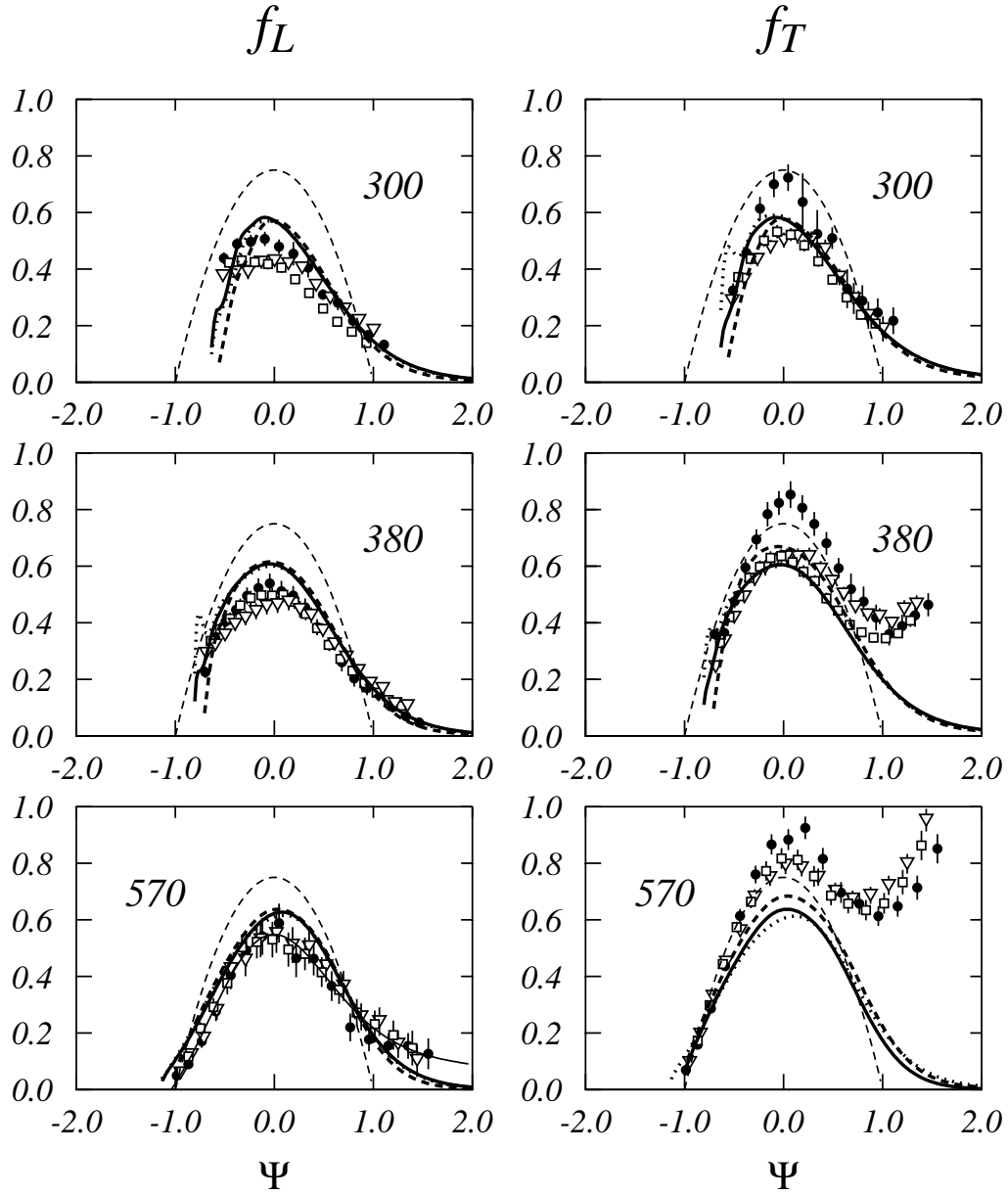


Figure 1: Empirical longitudinal,  $f_L$ , and transverse,  $f_T$ , scaling functions obtained from the experimental electromagnetic responses of Ref. [6]. The numbers in the panels indicate the values of the momentum transfer in MeV/c. The full circles refer to  $^{12}\text{C}$ , the white squares to  $^{40}\text{Ca}$ , and the white triangles to  $^{56}\text{Fe}$ . The thin black line in the  $f_L$  panel at 570 MeV/c, is the empirical scaling function obtained from a fit to the data. The thick lines show the results of our calculations when all the effects beyond the RFG model have been considered. The full lines have been calculated for  $^{12}\text{C}$ , the dotted lines for  $^{16}\text{O}$ , and the dashed lines for  $^{40}\text{Ca}$ . The dashed thin lines show the RFG scaling functions.

value of this index could be misleading if the responses have sharp resonances, we have also used the  $\mathcal{R}$  index which is instead sensitive to global properties of the differences between the functions. Since we know that the functions we want to compare are roughly bell shaped, we have inserted the factor  $1/f^{\max}$  to weight more the region of the maxima of the functions than that of the tails.

	$f_L$	
$q$ [MeV/c]	$\mathcal{D}$	$\mathcal{R}$
300	$0.107 \pm 0.002$	$0.152 \pm 0.013$
380	$0.079 \pm 0.003$	$0.075 \pm 0.009$
570	<b><math>0.101 \pm 0.009</math></b>	<b><math>0.079 \pm 0.017</math></b>
	$f_T$	
300	$0.223 \pm 0.004$	$0.165 \pm 0.017$
380	$0.235 \pm 0.005$	$0.155 \pm 0.014$
570	$0.169 \pm 0.003$	$0.082 \pm 0.007$

Table 1: Values of the  $\mathcal{D}$  and  $\mathcal{R}$  indexes, for the experimental scaling functions of Fig. 1.

In Tab. 1 we give the values of the indexes calculated by comparing the experimental scaling functions of the various nuclei at fixed value of the momentum transfer. We consider that the scaling between a set of functions is fulfilled when  $\mathcal{R} < 0.096$  and  $\mathcal{D} < 0.11$ . These values have been obtained by adding the uncertainty to the values of  $\mathcal{R}$  and  $\mathcal{D}$  for  $f_L$  at 570 MeV/c. From a best fit of this last set of data we extracted an empirical universal scaling function [7] represented by the thin full line in the lowest left panel of Fig. 1. This curve is rather similar to the universal empirical function given in Ref. [2].

Let's consider now the scaling of the theoretical functions. The thin dashed lines of Fig. 1 show the RFG scaling functions. The thick lines show the results of our calculations when various effects beyond the RFG are introduced, *i.e.*: nuclear finite size, collective excitations, final state interactions, and, in the case of the  $f_T$  functions, meson-exchange currents.

We have studied the effects of the nuclear finite size, by calculating scaling functions within a continuum shell model. At  $q=700$  MeV/c, these scaling functions are very similar to those of the RFG model. At lower values of the momentum transfer, the shell model scaling functions show sharp peaks, produced by the shell structure, not present in the RFG model. We found that shell model scaling functions fulfill the scaling of first kind, the most likely violated, down to 400 MeV/c.

We have estimated the effects of the collective excitations by doing continuum RPA calculations with two different residual interactions[8]. The RPA effects become smaller the larger is the value of the momentum transfer. At  $q > 600$  MeV/c, the RPA effects are negligible if calculated with a finite-range interaction. Collective excitations breaks scaling properties, but we found that scaling of first kind is satisfied down to about 500 MeV/c.

The presence of the MEC violates the scaling of the transverse responses. We

included the MEC by using the model of Ref. [9]. In our calculations only one-pion exchange diagrams are considered, including those with virtual excitation of the  $\Delta$ . In our model MEC effects start to be relevant for  $q \sim 600$  MeV/c. We found that MEC do not destroy scaling in the kinematic range of our interest.

The main modification of the shell model scaling functions, are produced by the FSI, we have considered by using the model developed in Ref. [8]. We obtained scaling functions very different from those predicted by the RFG model, and rather similar to the empirical ones. In any case, the FSI do not heavily break the scaling properties. We found that the scaling of first kind is conserved down to  $q=450$  MeV/c.

The same type of scaling analysis applied to  $(\nu_e, e^-)$  reaction leads to very similar results [7].

### 3 Superscaling Predictions

To investigate the prediction power of the superscaling hypothesis, we compared responses, and cross sections, calculated by using RPA, FSI and eventually MEC, with those obtained by using  $f_U^{\text{th}}$  and  $f_U^{\text{exp}}$ .

We show in Fig. 2 double differential electron scattering cross sections calculated with complete model (full) and those obtained with  $f_U^{\text{th}}$  (dashed lines) and  $f_U^{\text{exp}}$  (dotted lines). These results are compared with the data of Refs. [11, 12, 13].

The excellent agreement between the results of the full calculations and those obtained by using  $f_U^{\text{th}}$ , indicates the validity of the scaling approach in this kinematic region where the  $q$  values are larger than 500 MeV/c. The differences with the cross sections obtained by using the empirical scaling functions, reflect the differences between the various scaling functions shown in Fig. 1. The disagreement with the experimental data is probably due to the fact that our models do not consider the excitation of the real  $\Delta$  resonance, and the pion production mechanism.

The situation for the double differential cross sections is well controlled, since all the kinematic variables, beam energy, scattering angle, energy of the detected lepton, are precisely defined, and consequently also energy and momentum transferred to the target nucleus. This situation changes for the total cross sections which are of major interest for the neutrino physics. The total cross sections are only function of the energy of the incoming lepton, therefore they consider all the scattering angles and of the possible values of the energy and momentum transferred to the nucleus, with the only limitation of the global energy, and momentum, conservations. This means that, in the total cross sections, kinematic situations where the scaling is valid and also where it is not valid are both present.

We show in the first three panels of Fig. 3 various differential charge-exchange cross sections obtained for 300 MeV neutrinos on  $^{16}\text{O}$  target. In the panel (a) we show the double differential cross sections calculated for a scattering angle of  $30^\circ$ , as a function of the nuclear excitation energy. The values of the momentum transfer vary from about 150 to 200 MeV/c. This is not the quasi-elastic regime where the scaling is supposed to hold, and this explains the large differences between the various cross sections.

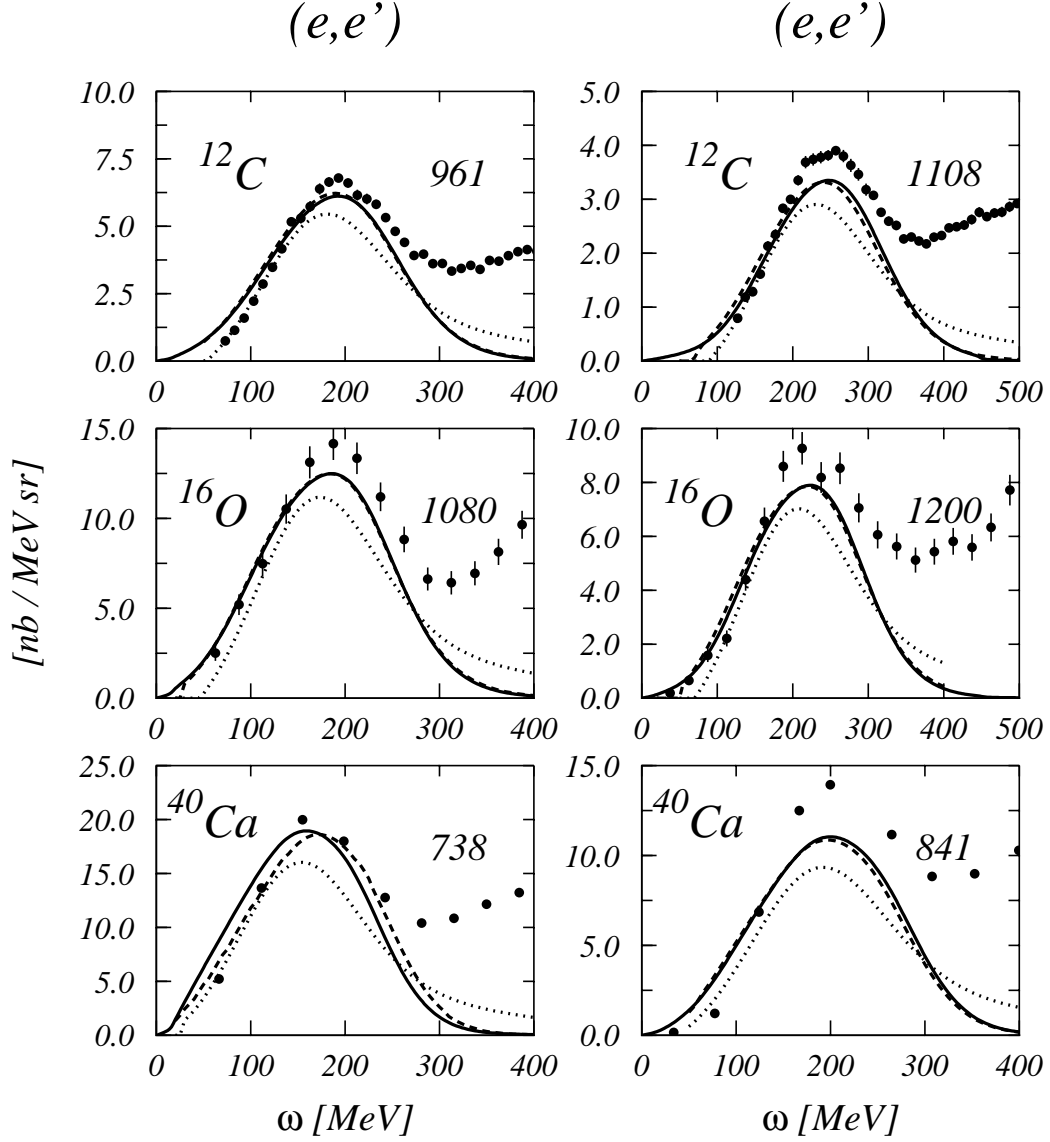


Figure 2: Inclusive electron scattering cross sections. The numbers in the panels indicate, in MeV, the energy of the incoming electron. The  $^{12}C$  data [11] have been measured at a scattering angle of  $\theta=37.5^\circ$ , the  $^{16}O$  data [12] at  $\theta=32.0^\circ$  and the  $^{40}Ca$  data [13] at  $\theta=45.5^\circ$ . The full lines show the results of our complete calculations. The cross sections obtained by using  $f_U^{th}$  are shown by the dashed lines, and those obtained with  $f_U^{ex}$  by the dotted lines.

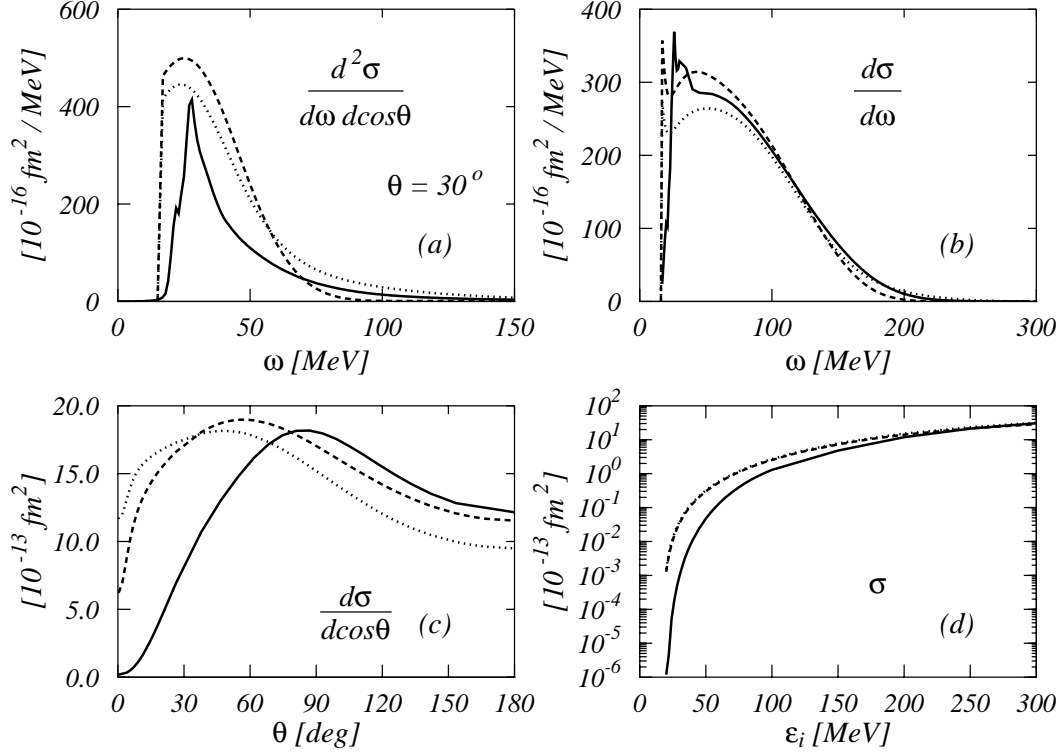


Figure 3: Neutrino charge exchange cross sections on  $^{16}\text{O}$ . In all the panels the full lines show the result of our complete calculation, the dashed (dotted) lines the result obtained with our universal (empirical) scaling function. The results shown in panels (a), (b) and (c) have been obtained for neutrino energy of 300 MeV. Panel (a): double differential cross sections calculated for the scattering angle of  $30^\circ$  as a function of the nuclear excitation energy. Panel (b): cross sections integrated on the scattering angle, always as a function of the nuclear excitation energy. Panel (c): cross sections integrated on the nuclear excitation energy, as a function of the scattering angle. Panel (d): total cross sections, as a function of the neutrino energy.

The cross sections integrated on the scattering angle are shown as a function of the nuclear excitation energy in the panel (b) of the figure, while the cross sections integrated on the excitation energy as a function of the scattering angle are shown in the panel (c). The first three panels of the figure illustrate in different manner the same physics issue. The calculation with the scaling functions fails in reproducing the results of the full calculation in the region of low energy and momentum transfer, where surface and collective effects are important. This is shown in panel (b) by the bad agreement between the three curves in the lower energy region, and in panel (c) at low values of the scattering angle, where the  $q$  values are minimal.

Total charge-exchange neutrino cross sections are shown in panel (d) as a function of the neutrino energy  $\epsilon_i$ . The scaling predictions for neutrino energies up to 200 MeV are unreliable. These total cross sections are dominated by the giant resonances, and more generally by collective nuclear excitation. We have seen that these effects strongly violate the scaling. At  $\epsilon_i = 200$  MeV the cross section obtained with our universal function is still about 20% larger than those obtained with the full calculation. This difference becomes smaller with increasing energy and is about the 7% at  $\epsilon_i = 300$  MeV. This is an indication that the relative weight of the non scaling kinematic regions becomes smaller with the increasing neutrino energy.

## References

- [1] W. M. Alberico, A. Molinari, T. W. Donnelly, E. L. Kronenberg and J. W. V. Orden, *Phys. Rev. C* **38**, p. 1801 (1988).
- [2] C. Maieron, T. W. Donnelly and I. Sick, *Phys. Rev. C* **65**, p. 025502 (2002).
- [3] J. E. Amaro, M. B. Barbaro, J. A. Caballero, T. W. Donnelly, A. Molinari and I. Sick, *Phys. Rev. C* **71**, p. 015501 (2005).
- [4] J. E. Amaro, M. B. Barbaro, J. A. Caballero, T. W. Donnelly and C. Maieron, *Phys. Rev. C* **71**, p. 065501 (2005).
- [5] T. W. Donnelly and I. Sick, *Phys. Rev. C* **60**, p. 065502 (1999).
- [6] J. Jourdan, *Nucl. Phys. A* **603**, p. 117 (1996).
- [7] M. Martini, G. Co', M. Anguiano and A. M. Lallena, *submitted for publication to Phys. Rev. C* (2006).
- [8] A. Botrugno and G. Co', *Nucl. Phys. A* **761**, p. 203 (2005).
- [9] M. Anguiano, G. Co', A. M. Lallena and S. R. Mokhtar, *Ann. Phys. (N.Y.)* **296**, p. 235 (2002).
- [10] G. Co', K. F. Quader, R. D. Smith and J. Wambach, *Nucl. Phys. A* **485**, p. 61 (1988).
- [11] R. M. Sealock *et al.*, *Phys. Rev. Lett.* **62**, p. 1350 (1989).



[12] M. Anghinolfi *et al.*, *Nucl. Phys. A* **602**, p. 405 (1996).

[13] C. Williamson *et al.*, *Phys. Rev. C* **56**, p. 3152 (1997).